Simulations of mono-sized solid particles in the Reflux Classifier under continuous process conditions

Naveedul Hasan Syed, Naseer Ahmed Khan

Department of Chemical Engineering, University of Engineering and Technology Peshawar Pakistan

Corresponding author: syednaveed@uetpeshawar.edu.pk (Naveedul Hasan Syed)

Abstract: In this study, a fluidized bed separator incorporating inclined channels, the Reflux Classifier (RC), was modeled to describe the transport behavior of mono-sized solid particles using a 2D computational segregation-dispersion model. The model is a volume flux-based model comprising the dispersion and segregation fluxes. Simulations were performed to examine variations in the solid volume fraction of particle species of size 0.163 mm and density 2450 kg/m³ by altering variables such as fluidization velocity, underflow rate and water flux in the feed. The system achieved a maximum solid volume fraction of 0.50 (v/v) near the base at a fluidization velocity 0.00020 m/s, that reduced to 0.20 at the fluidization velocity 0.0060 m/s. Overall, the results showed a decrease in the average solid volume fraction from 0.37 to 0.21 for the corresponding fluidization velocities. Simulation results also successfully demonstrated the capacity of the RC in retaining the solid particles at a superficial fluidization velocity 0.020 m/s, significantly higher than the terminal settling velocity, 0.015 m/s, of the solid particles, due to the presence of an inclined channel. Similarly, with increasing the underflow rate, the average solid volume fraction decreased from 0.29 to 0.055 due to the discharge of a larger quantity of solid particles from the base. Furthermore, a higher concentration of solid particles was observed in the inclined section at lower water flux in the feed stream. Additionally, flux balance calculations were carried out at different points within the RC to ensure the accuracy of the model predictions.

Keywords: beneficiation, fluidized beds, inclined channels, segregation, superficial velocity

1.   Introduction

Liquid Fluidization and sedimentation are fundamentally similar processes (Richardson and Zaki, 1954) in which a solid phase is in contact with a liquid phase to form a solid-liquid suspension (Di Felice, 2007). These processes have been widely used in industries including coal beneficiation, mineral processing, wastewater treatment, catalytic cracking, and gas purification (Epstein, 2005; Escudie et al., 2006; Mukherjee et al., 2009; Jemwa et al., 2012). In liquid fluidization solid particles are segregated based on the difference in their size and/or density by passing a fluidization liquid through a bed of solids, whereas, in sedimentation, a solid-liquid mixture is allowed to stay in a settling tank where solid particles settle down leaving behind a clear water (Richardson and Zaki, 1954; Rasul et al., 2000; Asif, 2004).

Improved and good separation quality is always the main aim in fluidization processes. Similarly, in sedimentation, researchers always work for the improvement in the settling rate of solid particles. Consequently, the researchers started focusing on the improvement of the designs of fluidized bed separators and settling tanks leading to the identification of an improved settling mechanism termed as the *Boycott effect* (Boycott, 1920; Ponder, 1925; Law et al., 1988; Masliyah et al., 1989; Nguyentranlam and Galvin, 2001). According to the *Boycott effect* (Boycott, 1920), segregation and/or sedimentation of solid particle species can be improved using inclined channels. These inclined channels provide a larger effective settling area for solid particles and hence improve their settling rate compared to vertical channels (Boycott, 1920; Ponder, 1925; Thompson and Galvin, 1997).

Various researchers carried out theoretical and experimental studies to understand the mechanism of segregation and settling in fluidized beds (Patel et al., 2008; Peng et al., 2016; Khan et al., 2017; Abbasfard et al., 2018) and inclined channels (Davis et al., 1989; Masliyah et al., 1989; Davis and Gecol, 1996; Nelson and Galvin, 1997). Nguyentranlam and Galvin (2001) developed for the first time a modified fluidized bed with a set of parallel inclined channels above it, named the Reflux Classifier (RC). The RC is a compact device, provides uniform feed distribution within the inclined channels and has been utilized in coal and mineral processing industries for separating valuable minerals from gangue (Galvin et al., 2002, 2005, 2010; Hunter et al., 2016). In the RC, the fluidization section separates solid particles similar to liquid fluidized beds, whereas the inclined channels act as highly efficient classification zones based on the principle of the *Boycott Effect* (Boycott, 1920). A schematic diagram of the RC is shown in Fig. 1.
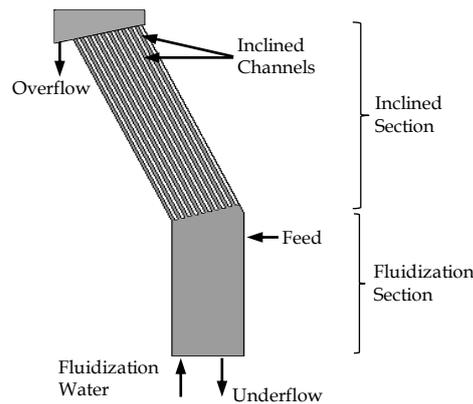
Fig. 1. Schematic of the Reflux Classifier

To understand the transport mechanism of solid particles in the RC, less amount of theoretical work has been done so far. Galvin and Nguyentranlam (2002) proposed a kinematic model based on the Ponder (1925) and Nakamura and Kuroda (1937) approaches to explain the process of sedimentation in inclined channels. Doroodchi et al. (2004) further modified the kinematic model of Galvin and Nguyentranlam (2002) by including the influence of a sediment layer in the inclined channel. The authors described the suspension profiles of mono-sized and binary particles within the inclined channel. Similarly, Doorodchi et al. (2005) used CFD approach to study the expansion of mono-sized and binary particles within the RC under batch process conditions. Li et al. (2017) proposed a model to describe the trajectory of a single particle in an inclined channel, which was further improved by Li et al. (2018) explaining the steady-state interactions between the fluidization and the segregation of mono-sized and binary suspensions in the inclined channel. The authors used the Richardson and Zaki (1954) hindered settling function for particles to describe transport behavior of particle species within the inclined channel (Li et al., 2018a, b). However, these studies were carried out for batch processes. Similarly, the contribution of dispersion in studying the transport behavior of particle species was not considered during the studies carried out by Doorodchi et al. (2004, 2005).

Syed Naveed et al. (2015) proposed for the first time a continuum model of the RC based on Kennedy and Bretton (1966) approach and demonstrated segregation of binary particle species. Syed et al. (2018) modified the continuum model and developed a complete 2D computational segregation-dispersion model to study the transport mechanism of multicomponent species within the RC under continuous process conditions. The model described the transport behavior of solid particles as a function of the segregation and dispersion fluxes. The Richardson and Zaki (1954) and Asif (1997) hindered settling models were incorporated to show segregation of particle species based on difference in their sizes (Syed Naveed et al., 2015; Syed, 2017) and densities (Syed et al., 2018). The model predictions of Syed et al. (2018) were validated with the published experimental results of Galvin et al. (2010) for a complex multicomponent system and were found in a good agreement.

In this study, the 2D segregation-dispersion model of the RC is used again to study theoretically the transport mechanism of mono-sized solid particles under continuous process conditions. The transport

behavior of mono-sized solid particles is explained by demonstrating variations in the volume fraction and net flux of solid particles within the RC under different operating conditions. Moreover, the predictions of the 2D model have been used to illustrate the capacity of the RC in retaining the solid particles at a higher superficial fluidization velocity due to the presence of an inclined channel. The study is useful in understanding the movement and sedimentation of solid particles within the fluidization and inclined sections of the RC and provides a basis for studying binary and multicomponent systems.

2. Theoretical model

A segregation-dispersion model based on the Kennedy and Bretton (1966) approach states that the net flux of a particle species at any location within a vessel consists of dispersion and segregation fluxes. According to 2D segregation-dispersion model (Syed et al., 2018), for the Reflux Classifier, the net flux of the particle species relative to a vessel has x and y components given as,

$$N_{x,i} = \phi_i u_{p\_x,i} = -D_{x,i}\frac{\partial \phi_i}{\partial x} + \phi_i u_{seg\_x,i} \tag{1}$$

$$N_{y,i} = \phi_i u_{p\_y,i} = -D_{y,i}\frac{\partial \phi_i}{\partial y} + \phi_i u_{seg\_y,i} \tag{2}$$

where N_x, N_y, u_{p_x}, u_{p_y}, u_{seg_x}, u_{seg_y}, D_x, D_y, represents the x and y components of net flux, particle velocity, segregation velocity relative to the vessel and dispersion coefficient, respectively. ϕ_i is the solid volume fraction of particle species i. Similarly, $-D_i\frac{\partial \phi_i}{\partial x}$ and $-D_i\frac{\partial \phi_i}{\partial y}$ are the dispersion fluxes in the x and y directions, respectively, whereas $\phi_i u_{seg\_x,i}$ and $\phi_i u_{seg\_y,i}$ are the segregation fluxes in the x and y directions, respectively.

A detailed description of the algorithm of the 2D model can be seen in Syed et al. (2018). However, a brief description of the model has been provided here.

In a continuous process, solids and liquid enters the system through the inlet and leave the system via the underflow and overflow. Therefore, the total volume flux, u_n, within the computational domain at the feed point and above is given as (Syed et al., 2018),

$$u_n = u_{fs} + N_f - N_u = u_f\phi_f + \sum \phi_i u_{p,i}. \tag{3}$$

Likewise, below the feed point the total volume flux is given as,

$$u_n = v_{fs} - N_u = u_f\phi_f + \sum \phi_i u_{p,i} \tag{4}$$

where, u_{fs} is the superficial fluidization velocity, u_f the interstitial fluid velocity, N_f is the feed flux, N_u is the underflow flux and ϕ_f is the voidage.

The segregation fluxes are written as a function of the slip velocities given as,

$$u_{seg\_x,i} = u_{slip\_x,i} + u_{f\_x} \tag{5}$$

$$u_{seg\_y,i} = u_{slip\_y,i} + u_{f\_y} \tag{6}$$

where $u_{slip\_x,i}$ and $u_{slip\_y,i}$ are the slip velocities of the particle species relative to the fluid in the x and y directions, respectively. Likewise, u_{f_x} and u_{f_y} are the interstitial fluid velocities in the x and y directions, respectively.

The x and y components of the slip velocity are calculated using the Richardson and Zaki (1954) hindered settling model represented as,

$$u_{slip\_x,i} = \left[u_{t,i}(1-\phi_t)^{n_i-1}\right]cos\theta \tag{7}$$

$$u_{slip\_y,i} = \left[u_{t,i}(1-\phi_t)^{n_i-1}\right]sin\theta \tag{8}$$

where $u_{t,i}$, ϕ_t and n are the terminal velocity, total solid volume fraction (v/v) and the Richardson and Zaki (1954) exponent, respectively.

The boundary condition at the base and outlet (overflow) are given as:

$$y = y_{max} \qquad\qquad \frac{\partial \phi_i}{\partial y} = 0 \tag{9}$$

$$y = 0 \qquad\qquad N_{y,i} = N_u . \tag{10}$$

2.1. Simulation details

Simulations were performed to study the influence of variables such as fluidization velocity, underflow rate and water flux in the feed stream on the transport behavior of mono-sized particles in the Reflux Classifier (RC) under continuous process conditions. The input variables such as particle properties, fluidization velocity, underflow rate and feed flux were specified from the beginning of the simulations. A particle size 0.163 mm as used by Moritomi et al. (1986) and Patel et al. (2008) was selected during the study and its properties are given in Table 1.

Table 1. Properties of mono-sized solid particle based on the data shown by Moritomi et al. (1986)

Particle density (kg/m³)	Particle size (m)	Terminal velocity (m/s)	Particle Reynolds number (Re_p)	Exponent n	Minimum fluidization velocity (m/s)
2450	0.000163	0.015	2.45	4.0	0.00020 m/s

A fixed value of 0.00030 m²/s for the dispersion coefficients, D_x, D_y, was used as a fitting parameter (Juma and Richardson, 1983; Asif and Petersen, 1993; Syed et al., 2018). The whole domain of the RC was discretized into equally spaced 200 shells and 21 elements in the x and y directions, respectively (Syed, 2017), as shown in Fig. 2. Element 1 is nearest to the upwards facing wall of the inclined channel, whereas element 21 is closest to the upper wall of the channel. Only one inclined channel of length 1 m and an angle of inclination of 70^0 with respect to the horizontal was considered during the simulations. Similarly, the height, h, of the lower section, i.e. fluidization section was taken as 1 m and the width, k, was taken as 0.006 m, whereas, the width of the inclined channel was obtained as $ksin\theta$ (Syed et al., 2018). The feed inlet point was kept at a height of 0.8 m (shell 80) and outlet was taken at a height of 1.95 m (shell 195).

In this study, mono-sized solid particles were used, therefore the solid particles moved according to the input variables. For example, if the fluidization velocity was high, all the solid particles moved upwards, whereas, in case of lower fluidization velocity the particle species moved downwards. The terms, segregation flux, in Eq. 1&2 were calculated from Eq. 5&6, respectively once the solid volume fraction was obtained. Now, if the solid particles move upwards, a volume of particles species equal to $\phi_i u_{seg\_y,i} A\Delta t$ will move from shell m to m+1. In contrast, if the solid particles move downwards, a volume of particles species equal to $\phi_i u_{seg\_y,i} A\Delta t$ will move from shell m to m-1 (Syed et al., 2018).

Similarly, the term dispersion flux in Eq. 1 was calculated using the finite difference method. For the concentration gradient having a negative value, the dispersion flux will become positive and solid particles will move in the axial direction (y direction) from shell m to m+1. Whereas, in case of a positive gradient, the dispersion flux will become negative and solid particles will move from shell m to m-1 (Patel et al., 2008; Syed et al., 2018).
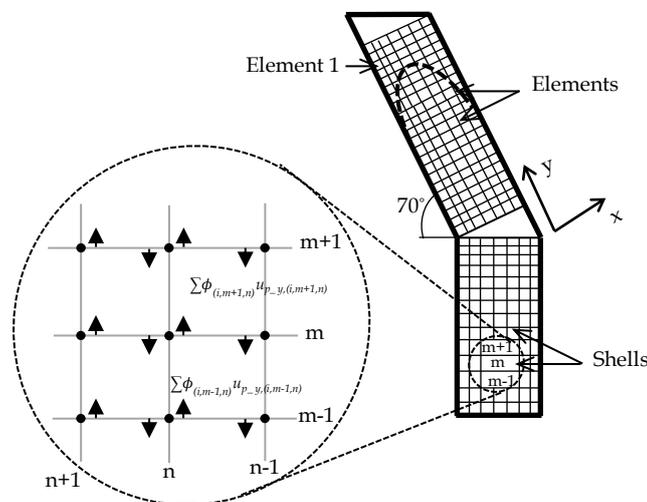
Fig. 2. Schematic diagram of the computational domain illustrating flux movement in the axial direction

3.   Results and discussion

3.1. Influence of the superficial fluidization velocity

Simulations were performed to examine the transport behavior of mono-sized solid particles in the Reflux Classifier (RC) at five different superficial fluidization velocities 0.00020, 0.00060, 0.0030, 0.0060 and 0.020 m/s, while the underflow rate was kept constant at 0.0020 m³/m²s. The feed flux was taken equal to 0.0080 m³/m²s comprising 0.0020 and 0.0006 m³/m²s of solids and water fluxes, respectively.

Fig. 3 shows the solid volume fractions of mono-sized solid particles versus height for the corresponding fluidization velocities in three distinct zones, fluidization, dilute and inclined zones at steady state in element 1. At first simulations were performed at a minimum superficial fluidization velocity 0.00020 m/s. The system achieved a maximum solid volume fraction of 0.49 near the base (black line). However, due to low fluidization velocity, the profile of the solid volume fraction in the fluidization zone was not smooth showing that the system was not fully fluidized. In contrast, the profile of the solid volume fraction in the dilute (at feed inlet and above) and inclined zones was smooth due to the hydraulic conveying of solid particles in the upward direction. In the inclined zone, the solid volume fraction reached to a maximum value of 0.31 (shell 140), showing that a relatively high number of solid particles settled down on the upward facing wall of the inclined channel while moving out via the overflow. A similar trend was observed in the fluidization zone for the second case when a superficial fluidization velocity of 0.00060 m/s was used (dashed dot line). However, in the dilute and inclined zones the solid volume fraction decreased comparatively. The solid volume fraction reached to a maximum value of 0.29 (shell 140) in the inclined section, demonstrating that more particles moved out in the overflow due to an increase in the superficial fluidization velocity.

In the third and fourth simulation runs, the superficial fluidization velocity was increased to 0.0030 and 0.0060 m/s, respectively. The system achieved maximum solid volume fractions of 0.33 (dash line) and 0.21 (small dash line) near the base at the corresponding superficial fluidization velocities. The profiles of the solid volume fractions were smooth in these cases illustrating that the system was fully fluidized. The solid volume fractions in the inclined section achieved the maximum values of 0.26 (shell 140) and 0.22 (shell 140) at the superficial fluidization velocities of 0.0030 and 0.0060 m/s, respectively showing that a higher number of solid particles moved out in the overflow with increasing fluidization velocity, as expected.

In the last run, a significantly higher superficial fluidization velocity of 0.020 m/s was used. This fluidization velocity was quite higher than the particle terminal settling velocity (Table 1). The results, represented by a dashed line, show that almost all the particles were pushed upwards and had a zero concentration in the fluidization zone. The feed slurry entered the inclined section at a superficial velocity of 0.026 m/s (fluidization + feed - underflow), however due to the inclination the solid particles settled down on the upward facing wall of the inclined channel and the solid volume fraction reached to a maximum value of 0.10 (shell 140) in the inclined section. The results demonstrated that even at a higher superficial velocity than the terminal settling velocity of the solid particles, the RC successfully retained the solid particles due to the presence of an inclined channel. These solid particles after settling on the inclined channel moved backwards, thus showing their presence in the dilute zone with a maximum value of the solid volume fraction of 0.12.
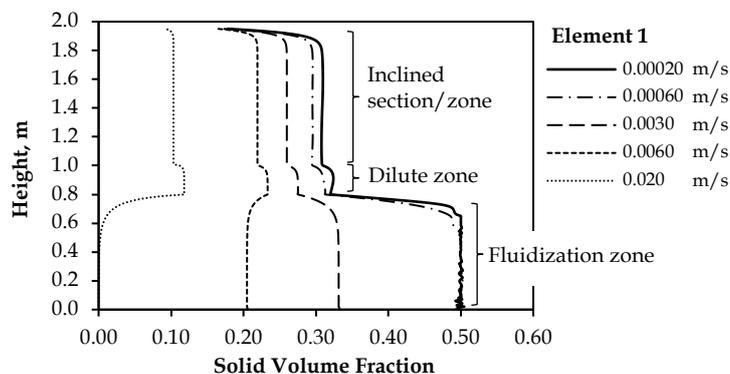
Fig. 3. Solid volume fraction versus height at superficial fluidization velocities ranging 0.00020 to 0.020 m/s

For keeping the things simple, results obtained from all the simulation runs are shown only for element 1, however some results describing the transport behavior of the solid particles at a superficial fluidization velocity of 0.0030 m/s in element 1, 11 and 21 are presented in Fig. 4. The results in Fig. 4 shows that the solid volume fraction remained same in the fluidization section in all the elements. In contrast, different concentration profiles were observed in the inclined section. Within the inclined section, the solid particles had a relatively higher volume fraction near the upward facing wall of the inclined channel, i.e. in element 1, however, the solid volume fraction decreased as the number of elements increased across the channel width. This is because solid particles were settling within the inclined channel.
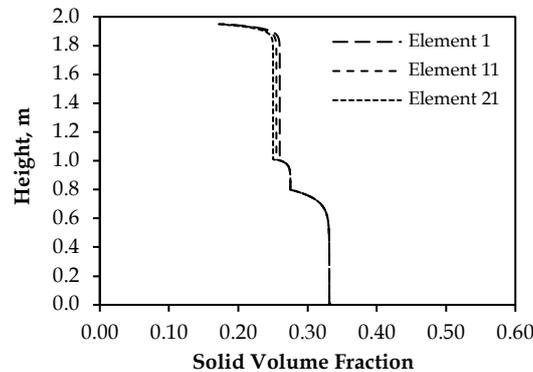
Fig. 4. Solid volume fraction versus height at a superficial fluidization velocity 0.0030 m/s

Fig. 5 shows the average solid volume fraction versus superficial fluidization velocity ranging 0.00020 to 0.0060 m/s. The results depict that the average solid volume fraction within the RC decreased from a value of 0.37 to 0.21 with increasing superficial fluidization velocity. The high hydraulic loadings pushed the solid particles upwards in the overflow. The trend of decrease in the average solid volume fraction predicted by the 2D model was found qualitatively similar to the experimental and modeling results of Doroodchi et al. (2004, Fig 3).
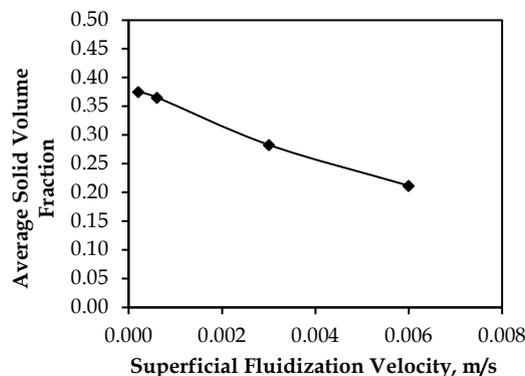
Fig. 5. Influence of superficial fluidization velocity (0.00020 - 0.0060 m/s) on the average solid volume fraction within the Reflux Classifier

Fig. 6 shows the net flux of mono-sized solid particles across the channel width at a height of 1.4 m (shell 140) for five different superficial fluidization velocities ranging 0.00020 to 0.020 m/s. In   Fig. 6, the net flux, with parabolic profiles, of mono-sized solid particles increased with increasing fluidization velocity. During the first two simulation runs, as discussed above, the system was not fully fluidized and the movement of solid particles through the system was very slow. This can be seen with the lower net flux values for the fluidization velocities 0.00020 and 0.00060 m/s (continuous and dash-dot curves). Moreover, both the curves overlap each other showing a little increase in the fluidization velocity had an almost negligible effect on the movement of the solid particles. On further increasing the fluidization velocity, the net flux through the inclined section increased gradually (dash, small-dash, and dotted curves).

Furthermore, the net flux near the walls of the channel (element 1 and 21) was negative, representing that the solid particles slide towards the fluidization section of the RC as was observed by Syed Naveed (2015) in the case of a binary system.
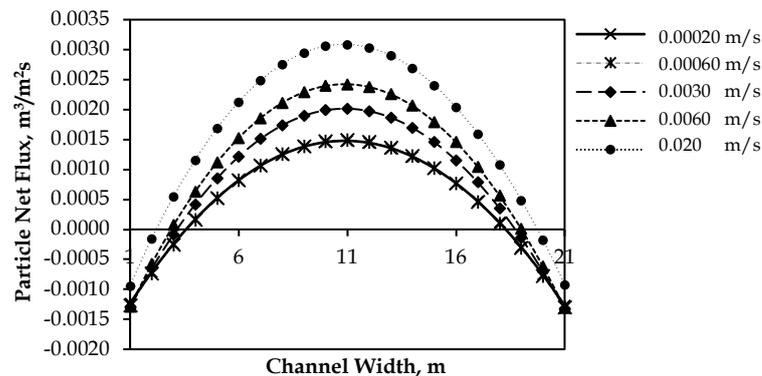
Fig. 6. Net flux of mono-sized particles versus channel width for the fluidization velocities ranging 0.00020 to 0.020 m³/m²s

Flux balance calculations were carried out to ensure mass conservation within the system. A sample of calculations have been provided in Appendix-A1.

3.2. Influence of underflow rate

Simulations were performed to examine the influence of underflow rate on the transport behavior of mono-sized particles in the Reflux Classifier (RC). Fig. 7 shows the solid volume fraction versus height for five sets of simulation runs carried out at the underflow rates ranging 0.00050 to 0.01 m³/m²s while keeping the superficial fluidization velocity and feed flux constant at 0.0030 m/s and 0.0080 m³/m²s, respectively.

The system achieved a maximum solid volume fraction of 0.33 in the RC in the first four runs at the underflow rates 0.00050, 0.0010, 0.0020 and 0.0040 m³/m²s. However, the solid volume fraction decreased with increasing the underflow rate in the inclined section and the dilute zone. In the final run, the underflow rate was increased to a higher value of 0.01 m³/m²s, that caused the maximum quantity of solid particles to discharge from the RC. The solid volume fraction was almost zero in the inclined section, whereas in the fluidization section a maximum value of solid volume fraction of 0.2 was reached.
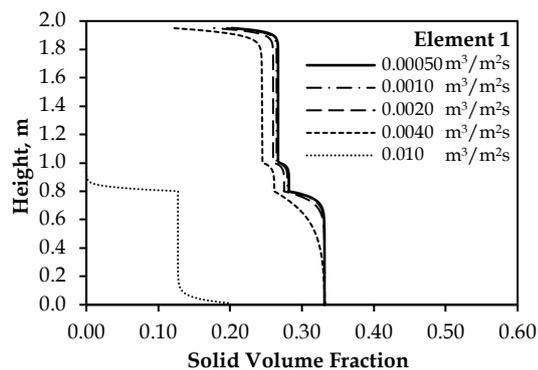
Fig. 7. Solid volume fraction versus height with changing underflow rate

Fig. 8 presents the average solid volume fraction versus underflow rate. The figure shows that average solid volume decreased from a value of 0.29 to 0.01 with increasing underflow rate. The increase in underflow rate pulled the solid particles downwards causing them to discharge from the base. At the underflow rate 0.01 m³/m²s, the solid particles discharged at a higher rate causing a significant decrease in the average solid volume fraction within the RC.
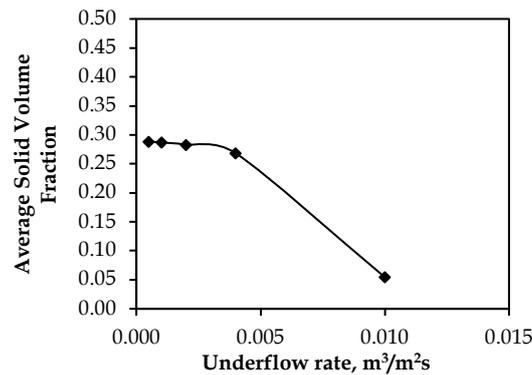
Fig. 8. The influence of underflow rate on the average solid volume fraction within the Reflux Classifier

3.3. Influence of water flux in feed stream

Fig. 9 demonstrate the solid volume fraction versus height for the changing water flux in the feed stream. The transport behavior of mono-sized solid particles was examined by increasing the water flux ranging 0.00050 to 0.020 m^3/m^2s while keeping the solid flux constant at 0.0020 m^3/m^2s in the feed stream. During the simulations, the underflow rate and superficial fluidization velocity were also kept constant at 0.0020 m^3/m^2s and 0.0030 m/s, respectively.

Fig. 9 illustrates that the maximum solid volume fraction near the base of the fluidization zone remained constant at 0.33 for the five sets of simulation runs. However, the solid volume fraction changed significantly in the dilute zone and inclined section of the Reflux Classifier (RC) with changing water flux. In the first run, a concentrated feed comprising water and solid fluxes of 0.00050 and 0.0020 m^3/m^2s, respectively was used. The results showed that the solid volume fraction in the inclined section was very high and reached to a maximum value of 0.48, whereas in the dilute section it attained a value of 0.49. This shows a very packed column and in general, the solid particles moved with a very low velocity within the RC.

In the next four runs, the water flux was increased gradually in the feed stream while keeping the solid flux constant. The figure shows that the solid volume fraction in the dilute and inclined sections of the RC decreased from relatively higher values of 0.49 to 0.097 in the dilute section and 0.48 to 0.088 in the inclined section. These results demonstrate that with higher values of water flux the superficial velocity (feed flux) increased at the inlet, thus causing the solid particles to move out via the overflow with relatively higher velocities. The results also showed the role of water in the feed stream while operating the RC. Usually, from the literature survey, it can be found that a pulp density of 45 to 50% has been used in most of the studies related to the RC (Galvin et al. 2005, 2010). This is because, in the RC, an autogenous dense medium is created to separate finer or low-density particles from the coarser or denser ones. To create an autogenous dense medium, low superficial fluidization velocity is preferred, therefore, water flux in the feed stream is adjusted in such a way as to satisfy the needs for hydraulic loadings.
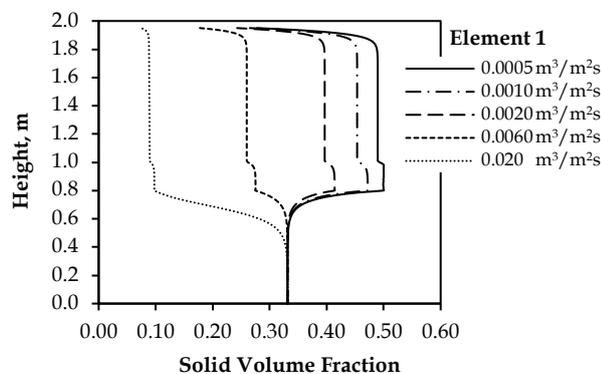
Fig. 9. Solid volume fraction versus height with increasing water flux in the feed stream while keeping the solid flux in the feed stream at 0.002 m^3/m^2s

Fig. 10 shows a decrease in the average solid volume fraction as a function of increasing water flux in the feed stream. The average solid volume fraction decreased from a relatively higher value of 0.42 to a relatively lower value of 0.17 with increasing water flux in the feed stream.
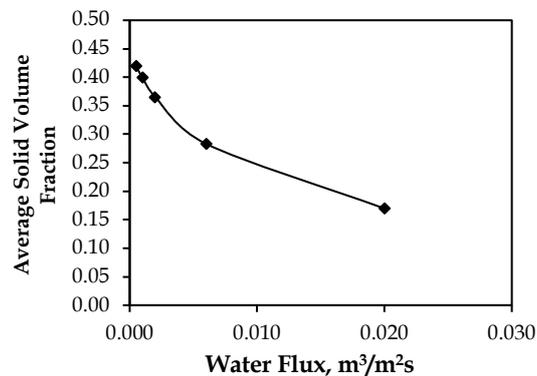
Fig. 10. The influence of water flux in the feed stream on the average solid volume fraction within the Reflux Classifier

4.   Conclusions

A 2D segregation-dispersion model of the Reflux Classifier (RC) was utilized to investigate the transport behavior of mono-sized solid particles within the RC. A systematic approach was adopted to carry out simulations while changing different variables such as superficial fluidization velocity, underflow rate and water flux in the feed stream. The predictions of the model were shown in the form of variations in the solid volume fraction within the RC with changing process conditions.

Study of the influence of fluidization velocity showed that the overall solid volume fraction decreased with increasing fluidization velocity and solid particles moved out via the overflow. It was demonstrated through the model predictions that at a significantly higher fluidization velocity of 0.020 m/s, the RC was able to retain solid particles with terminal settling velocity 0.015 m/s due to the presence of an inclined channel. The net flux movement within the RC at different fluidization velocities showed that the movement of particles increased with increasing hydraulic loadings. Moreover, the parabolic profile of the net flux showed that the velocity of solid particles was higher in the middle region while near the walls of the channel the velocities of the particles had negative values. The negative values represented that the solid particles moved backward in the fluidization section of the RC.

Similarly, with an increase in the underflow rate, the average solid volume fraction within the RC decreased due to solid particles discharging in the underflow. However, the influence of water flux in the feed stream showed significant changes in the solid volume fraction within the inclined section of the RC. At a lower water flux 0.00050 m³/m²s, the solid volume fraction had a relatively higher value of 0.48 in the inclined section that decreased to a value of 0.088 with an increase in the water flux to 0.020 m³/m²s.

Overall the model predictions provided a comprehensive description of the transport behavior of the mono-sized solid particles under different operating conditions.

Acknowledgments

Appendix-A1

Flux balance calculations were carried out at different points within the computational domain to ensure mass conservation within the system. The calculations were carried out in the fluidization zone i.e. below the feed inlet at shell 20, in the dilute zone i.e. above the feed point and below the inclined channel at shell 95, and in the inclined zone/section at shell 150. Eq. 1&2 were used to calculate the net

flux of the solid particles relative to the vessel. Similarly, Eq. 3&4 were used to calculate the total volume flux through the system. The total volume flux below the feed inlet using Eq. 4 was obtained equal to 0.0010 m³/m²s. Similarly, Eq. 1,2&4 were used to calculate the net flux through the system by the data generated through simulations that equals to 0.0010 m³/m²s. Hence the total flux within the system was balance. The calculations at different points within the computational domain of the RC are given below.

Fluidization velocity, u_{fs}	=	0.0030	m/s
Underflow flux, N_u	=	0.0020	m³/m²s
Volumetric flux of solid particle in feed, N_1	=	0.0020	m³/m²s
Volumetric flux of water in feed, N_w	=	0.0060	m³/m²s
Total feed flux, $N_f = N_1 + N_w$	=	0.0020 + 0.0060	
	=	0.0080	m³/m²s

Flux balance below the feed point (shell 20)

Total volume flux, $u_n = u_{fs} - N_u$	=	0.0030 - 0.0020	
	=	**0.0010**	**m³/m²s**

Component balance

Net flux, $u_n = u_f \phi_f + \sum \phi_i u_{p,i}$	=	(2.49e-3)x(1-0.33) +(-6.62e-4)	
	=	**0.0010**	**m³/m²s**

Flux balance in dilute zone (shell 95)

Total volume flux, $u_n = u_{fs} + N_f - N_u$	=	0.0030 + 0.0080 - 0.0020	
	=	**0.0090**	**m³/m²s**

Component balance

Net flux, $u_n = u_f \phi_f + \sum \phi_i u_{p,i}$	=	(1.05e-2)x(1-0.27) +(1.31e-3)	
	=	**0.0089**	**m³/m²s**

Flux balance in the inclined channel (shell 150)

Total volume flux, $u_n = u_{fs} + N_f - N_u$	=	0.0030 + 0.0080 - 0.0020	
	=	**0.0090**	**m³/m²s**

Component balance

Net flux, $u_n = u_f \phi_f + \sum \phi_i u_{p,i}$	=	(0.0134)x(1-0.26) +(-1.29e-3)	
	=	**0.0089**	**m³/m²s**

Nomenclature

A	projected area of the particle (m²)		*Greek letters*	
D	dispersion coefficient (m²/s)		ϕ	solid volume fraction
h	height of the fluidization section (m)		ϕ_t	total solid volume fraction
k	width of the fluidization section (m)		ϕ_f	voidage
N	net flux (m³/m²s)		μ	fluid viscosity (Pa s)
N_f	feed flux (m³/m²s)		ρ_f	liquid density (kg/m³)
N_w	volumetric flux of water in feed (m³/m²s)		ρ_p	particle density (kg/m³)
N_u	underflow flux (m³/m²s)			
n	Richardson Zaki exponent (dimensionless)		*Subscripts*	
RC	reflux classifier		*avg*	average
Re_p	particle Reynolds number (dimensionless)		*seg*	segregation
t	time (s)		f	liquid fluid
u_{fs}	superficial fluidization velocity (m/s)		i	ith particle
u_f	interstitial fluid velocity (m/s)		p	particle
u_p	particle velocity (m/s)		w	water
u_{seg}	segregation velocity of solid particles (m/s)			
u_t	terminal settling velocity of solid particles (m/s)			
u_n	total volume flux (m/s)			
u_{slip}	slip velocity of solid particles (m/s)			
x	lateral distance from wall			
y	vertical distance from the base			

References

ABBASFARD, H., EVANS, G.M., KHAN, M.S., MORENO-ATANASIO, R., 2018. *A new two-phase coupling model using a random fluid fluctuating velocity: application to liquid fluidized beds*. Chemical Engineering Science, 180, 79 – 94.

ASIF, M., 1997. *Modelling of multi-solid liquid fluidized beds*. Chemical Engineering Technology, 20, 485 – 490.

ASIF, M., 2004. *The complete segregation model for a liquid fluidized bed: formulation and related issues*. Powder Technology, 140, 21 – 29.

ASIF, M., and PETERSEN, J.N., 1993. *Particle dispersion in a binary solid–liquid fluidized bed*. A.I.Ch.E. Journal, 39 (9), 1465 – 1471.

BOYCOTT, A.E., 1920. *Sedimentation of blood corpuscles*. Nature, 104, 532.

DAVIS, R. H., and GECOL, H., 1996. *Classification of concentrated suspensions using inclined settlers*. International Journal of Multiphase Flow, 22 (3), 563 – 574.

DAVIS, R.H., ZHANG, X., AGARWALA, J.P., 1989. *Particle classification for dilute suspensions using an inclined settler*. Industrial and Engineering Chemistry Research, 28, 785 – 793.

Di FELICE, R., 2007. *Liquid suspensions of single and binary component solid particles-An overview*. China Particulogoy, 5, 312 – 320.

DOROODCHI, E., FLETCHER, D.F., GALVIN, K.P., 2004. *Influence of inclined plates on the expansion behaviour of particulate suspensions in a liquid fluidized bed*. Chemical Engineering Science, 59, 3559 – 3567.

DOROODCHI, E., GALVIN, K.P., FLETCHER, D.F., 2005. *The influence of inclined plates on expansion behavior of solid suspensions in a liquid fluidized bed – a computational fluid dynamics study*. Powder Technology, 160, 20 – 26.

EPSTEIN, N., 2005. *Teetering*. Powder Technology, 151, 2 – 14.

ESCUDIE, R., EPSTEIN, N., GRACEA, J.R., BIA, H.T., 2006. *Layer inversion phenomenon in binary-solid liquid-fluidized beds: Prediction of the inversion velocity*. Chemical Engineering Science, 61, 6667 – 6690.

GALVIN, K.P., CALLEN, A., ZHOU, J., DOROODCHI, E., 2005. *Performance of the reflux classifier for gravity separation at full scale*. Minerals Engineering, 18, 19 – 24.

GALVIN, K.P., DOROODCHI, E., CALLEN, A.M., LAMBERT, N., PRATTEN, S.J., 2002. *Pilot plant trial of the reflux classifier*. Minerals Engineering, 15, 19 – 25.

GALVIN, K.P., ZHOU, J., WALTON, K., 2010. *Application of closely spaced inclined channels in gravity separation of fine particles*. Minerals Engineering, 23, 326 – 338.

HUNTER, D. M., ZHOU, J., IVESON, S. M., GALVIN, K. P., 2016. *Gravity separation of ultra-fine iron ore in the Reflux Classifier*. Mineral Processing and Extractive Metallurgy, 125, 126 – 131.

JEMWA, G.T., ALDRICH, CHRIS, 2012. *Estimating size fraction categories of coal particles on conveyor belts using image texture modeling methods*. Expert Systems with Applications, 39, 7947 – 7960.

JUMA, A. K. A., and RICHARDSON, J. F., 1983. *Segregation and mixing in liquid fluidized beds*. Chemical Engineering Science, 38 (6), 955 – 967.

KENNEDY, S.C., and BRETTON, R.H., 1966. *Axial dispersion of spheres fluidized with liquids*. A.I.Ch.E. Journal, 12, 24 – 30.

KHAN, M.S., MITRA, S., GHATAGE, S.V., DOROODCHI, E., JOSHI, J.B., and EVANS, G.M., 2017. *Segregation and dispersion studies in binary solid-liquid fluidized beds: a theoretical and computational study*. Powder Technology, 314, 400 - 411.

LAW, H. S., MACTAGGART, R. S., NANDAKUMAR, K., MASLIYAH, J. H., 1988. *Settling behavior of heavy and buoyant particles from a suspension in an inclined channel*. Journal of Fluid Mechanics, 187, 301 – 318.

LI, Y., LI, N., Qi, X., ZHANG, W., ZHU, R., 2018b. A sedimentation model for particulate suspensions in liquid-solid fluidized beds with inclined channels. Physicochemical Problems of Mineral Processing, 54(3), 837 – 846.

LI, Y., LI, Y., XIA, W., HE, C., ZHU, R., 2017. *A novel particulate sedimentation model in inclined channels of liquid–solid fluidized bed*. Powder Technology, 305, 764 – 770.

LI, Y., Qi, X., LI, N., WANG, A., ZHANG, W., ZHU, R., Peng, Z., 2018a. Motion characterisitics of binary solids in a liquid fluidized bed with inclined plates. Particuology, 39, 48 – 54.

MASLIYAH, J. H., NASR-EL-DIN, H., NANDAKUMAR, K., 1989. *Continuous separation of bidisperse suspensions in inclined channels*. International journal of Multiphase Flow, 15 (5), 815 – 829.

MORITOMI, H., YAMAGISHI, T., CHIBA, T., 1986. *Prediction of complete mixing of liquid fluidized binary solid particles*. Chemical Engineering Science, 41, 297 – 305.

MUKHERJEE, A.K., MISHRA, B.K., KUMAR, R.V., 2009. *Application of liquid/solid fluidization technique in beneficiation of fines*. International Journal of Mineral Processing, 92, 67 – 73.

NELSON, D., LIU, J., and GALVIN, K.P., 1997. *Autogenous dense medium separation using an inclined counterflow settler*. Mineral Engineering, 10, 871 – 881.

NGUYENTRANLAM, G., GALVIN, K.P., 2001. *Particle classification in the reflux classifier*. Mineral Engineering, 14 (9), 1081 – 1091.

PATEL, B.K., RAMIREZ, W.F., GALVIN, K.P., 2008. *A generalized segregation and dispersion model for liquid fluidized beds*. Chemical Engineering Science, 63, 1415 – 1427.

PENG, Z., JOSHI, J.B., MOGHTADERI, B., KHAN, M.S., DOROODCHI, E., and EVANS, G.M., 2016. *Segregation and Dispersion of Binary Solids in Liquid Fluidized Beds: a CFD-DEM Study*. Chemical Engineering Science, 152, 65 – 83.

PONDER, P., 1925. *On sedimentation and Rouleaux formation*. Quarterly journal of experimental physiology, 15, 235 – 252.

RASUL, M.G., RUDOLPH, V., WANG, F.Y., 2000. *Particles separation using fluidization techniques*. International Journal of Mineral Processing, 60, 163 – 179.

RICHARDSON, J.F., and ZAKI, W.N., 1954. *Sedimentation and fluidization: Part I*. Transactions of the Institution of Chemical Engineers, 32, 35 – 53.

SYED NAVEED, DICKINSON, J., GALVIN, K.P., MORENO-ATANASIO, R., 2015. *A continuum simulation model for the reflux classifier*. APCChE 2015 Congress, Chemeca 2015, Melbourne, Sept 27 – 01 Oct.

SYED, N.H., 2017. *A continuous, dynamic and steady state segregation-dispersion model of the reflux classifier*. PhD Thesis, The University of Newcastle, NSW, Australia.

SYED, N.H., DICKINSON, J.E., GALVIN, K.P., MORENO-ATANASIO, R., 2018. *Continuous, dynamic and steady state simulations of the reflux classifier using a segregation-dispersion model*. Minerals Engineering, 115, 53 – 67.

THOMPSON, P.D., and GALVIN, K.P., 1997. *An empirical description for the classification in an inclined counter-flow settler*. Minerals Engineering, 10, 97 – 109.